1989ApJ...337..382P

THE ASTROPHYSICAL JOURNAL, 337:382–398, 1989 February 1
© 1989. The American Astronomical Society. All rights reserved. Printed in U.S.A.

FAST WINDS FROM THE CENTRAL STARS OF NGC 6543 AND NGC 6826[1]

M. PERINOTTO
Istituto di Astronomia, Università di Firenze
M. CERRUTI-SOLA
Osservatorio Astrofisico di Arcetri, Firenze
AND
H. J. G. L. M. LAMERS
SRON Laboratory for Space Research and Astronomical Institute, Utrecht
Received 1988 February 2; accepted 1988 June 15

ABSTRACT

The central stars of the planetary nebulae NGC 6543 and NGC 6826 have been investigated for the properties of their fast winds. With low- and high-resolution *IUE* data, together with other observations, the fundamental parameters of the central stars, needed for the wind's analysis, have been estimated.

Using the SEI method, the properties of the fast winds have been analyzed and the associated mass-loss rates determined. These amount to $\dot{M} = (4.0^{+10}_{-2.1}) \times 10^{-8}$ and $(5.2^{+34}_{-4.5}) \times 10^{-8}$ $M_\odot$ yr^{-1} for NGC 6543 and NGC 6826, respectively. These values have been compared with determinations obtained by other authors.

A comparison with the behavior of Population I OB stars suggests that the same mass-loss mechanism dominating in young OB stars is likely to be responsible for the fast winds observed in the central stars of these planetary nebulae.

Subject headings: nebulae: individual (NGC 6543, NGC 6826) — nebulae: planetary — stars: mass loss — stars: winds — ultraviolet: spectra

I. INTRODUCTION

The structure of the outer atmosphere of central stars of planetary nebulae (PNCSs) is at present best studied using UV lines observed with the *IUE* satellite. The instrument works in the spectral range 1150–3200 Å at low resolution (6 Å) or high resolution (0.15 Å). The low-resolution *IUE* spectra are adequate to reveal P Cygni–type features (see Heap *et al.* 1978) but fail to detect a wind if the profile is essentially in emission, as in Wolf-Rayet stars, or is dominated by a blueshifted absorption (Cerruti-Sola and Perinotto 1985, hereafter CP). The low-resolution spectra are also useful for measuring the terminal velocity of the winds and for a first approximate determination of their mass-loss rates. The high-resolution *IUE* spectra are entirely adequate to study in detail the whole line profile, but they can be used only in objects bright enough to give a measurable stellar continuum.

A study of a large sample of PNCSs with low-resolution *IUE* spectra has been made by CP, while investigations of individual objects have been done with low or high resolution by various authors. The main results from these studies are that the phenomenon of stellar winds is quite common among PNCs with edge velocity ranging from 1000 to 5000 km s^{-1} and mass-loss rates ranging from 5×10^{-11} to 2×10^{-6} $M_\odot$ yr^{-1}. However, these determinations of mass-loss rates ($\dot{M}$) are rather inaccurate because of uncertainties related to the different procedures used to interpret the observations, because of the use in various objects of low-resolution data, and because of uncertainties in the knowledge of the stellar parameters needed to deduce $\dot{M}$.

On the other hand, the knowledge of the mass-loss rates in PNCSs is important to study their effect on the evolution of the central stars, and on the genesis and dynamics of the nebulae. It is important also for extending the investigation of stellar winds to hot stars with fundamental parameters much different from those of Population I OB stars, thereby contributing to a better understanding of the mechanisms which produce winds in hot stars.

With this work we study with high- and low-resolution *IUE* spectra the central stars of the planetary nebulae NGC 6543 and NGC 6826. The observed line profiles are interpreted by means of line fitting with profiles calculated with a method recently developed by us (Lamers, Cerruti-Sola, and Perinotto 1987, hereafter LCP). This method (Sobolev with exact integration [SEI]) is based on the calculation of the source function with the Sobolev approximation combined with an exact solution of the radiative transfer equation. In § II we determine the stellar parameters, in particular those needed for the application of the SEI method: chemical composition, stellar temperature, and radius. In § III we study the wind properties and determine their mass-loss rates. The conclusions follow in § IV.

II. STELLAR PARAMETERS

a) Chemical Abundances

For chemical abundances we cannot do better at present than use the abundances observed in the nebula, because abundances in the stellar atmosphere are not available for NGC 6543 and NGC 6826. That may not be entirely adequate because, according to the predictions of the stellar evolution theory, particularly He, C, and N are expected to suffer substantial changes during the evolutionary phases which precede the arrival of the star at the tip of the asymptotic giant branch (AGB) in the H-R diagram (see Iben and Renzini 1983). Therefore, depending on the initial mass of the progenitor, the chemical abundances of H, C, N prevailing in the nebulae may be quite different from the corresponding values in the remnant

[1] Based on data from the *International Ultraviolet Explorer*, from the Archives of the Villafranca Station of the European Space Agency.

© American Astronomical Society • Provided by the NASA Astrophysics Data System

1989ApJ...337..382P

star and in its wind. This, however, is not the case for oxygen, because its abundance is not expected to change much during the mentioned evolutionary phases.

To have the best determinations of nebular abundances in NGC 6543 and NGC 6826, we have searched for all papers dealing with the subject using UV, optical, or IR data, starting with the fundamental work of Torres-Peimbert and Peimbert (1977) up until the present. Thus all the modern photoelectric work is considered, as well as the relevant work made before our starting date, because various authors most active in the field have thereafter summarized their previous determinations.

The adopted abundances are given in Table 1, where solar abundances are also shown for comparison. Measurements by different authors are quite close to each other except for carbon. For NGC 6543, Aller and Czyzak (1983) give C/H = 13×10^{-4}, which they consider to be of low reliability, while Kaler (1981*a*) has 2.4×10^{-4} and Pwa, Mo, and Pottasch (1984) have 2.3×10^{-4}. Kaler used faint optical lines of carbon (whose origin is not entirely known), and obtains its abundance from a scaling procedure with other nebulae where both optical lines and strong collisionally excited UV lines had been measured. This abundance is close to that found by Pwa *et al.*, who use an entirely new technique, i.e., the narrow absorption component in the main P Cygni profiles. The abundance of silicon is assumed to be equal to the solar one for lack of determinations in our stars.

Apart from carbon and silicon, the accuracy of abundances of the heavy elements in Table 1 should be better than a factor of 2. We consider our adopted nebular abundances to be accurate as follows: He by 10%, C by a factor of 2, Si by the same factor (the silicon-to-oxygen ratio should not differ significantly from the solar value) and N, O, Ne by a 40%. When applying these abundances to the stellar winds, no extra uncertainty is to be added for O, Ne, and Si, while an extra error is likely to occur for He, C, N in the sense that nebular abundances of these elements may underestimate their counterparts in the wind.

b) *Effective Temperature*

To obtain $T_{\rm eff}$, we use the Zanstra method, looking for the best solution which at the same time reproduces the observed continuum stellar flux.

TABLE 1

ADOPTED CHEMICAL ABUNDANCES

Ratio	NGC 6543	Sources	NGC 6826	Sources	Sun	Sources
He/H	0.11	1, 2	0.106	1, 2, 7	0.085	8
C/H	5.9(−4)[a]	2, 3, 4	1.3(−3)[b]	2, 3, 7	4.7(−4)	9
N/H	8.7(−5)	2	3.0(−5)	2	9.8(−5)	9
O/H	5.6(−4)	2, 5	2.9(−4)	2, 5	8.3(−4)	9
					2.8(−4)[c]	10
Ne/H	1.4(−4)	2, 6	7.0(−5)	2, 6	4.5(−5)[c]	10
Si/H	3.3(−5)[d]	...	3.3(−5)[d]	...	3.3(−5)	8

NOTE.—Parentheses enclose powers of factor 10.

[a] Sources 2, 3, and 4 give 1.3(−3), 2.4(−4), and 2.3(−4), respectively.

[b] Sources 2, 3, and 7 give 1.7(−3), 1.5(−4), and 8.9(−4). We retain only sources 2 and 7.

[c] Coronal values.

[d] Not measured. Assumed equal to the solar abundances.

REFERENCES.—(1) Kaler 1978*b*; (2) Aller and Czyzak 1983; (3) Kaler 1981*a*; (4) Pwa, Mo, and Pottasch 1984; (5) Kaler 1978*a*; (6) Pottasch *et al.* 1986; (7) French 1983; (8) Allen 1973; (9) Lambert 1978; (10) Parkinson 1977.

i) *Zanstra Temperatures*

Following Bohlin, Harrington, and Stecher (1982), we define, for a stellar flux distribution $F(\nu)$, the dimensionless parameter

$$Q(\lambda_0, \lambda_*) = h \int_{\nu_0}^{\infty} [F(\nu)/h\nu] d\nu / F(\nu_*) , \qquad (1)$$

where λ_* is a reference wavelength and the integral is the total number of photons beyond ν_0. The quantity Q can be readily obtained for a blackbody or for a stellar atmosphere model and is related to observable quantities. In fact, with λ_0 taken as the hydrogen ionization threshold 912 Å, Q can be related to the luminosity of the nebula at Hβ. If λ_0 is the He^+ ionization limit 228 Å, Q can be related to a recombination line of He^+. By choosing λ_* as 1300 Å and again following Bohlin, Harrington, and Stecher (1982), we obtain the equations

$$\log [\eta_{\rm H^0} Q(912, 1300)] = -1.61 - 1.49 c_\beta + 0.04 \log (10^{-4} T_e) + \log F({\rm H}\beta)_{\rm obs} - \log F^*(1300)_{\rm obs} , \qquad (2)$$

$$\log [\eta_{\rm He^+} Q(228, 1300)] = -1.94 - 0.33 c_\beta + 0.3 \log (10^{-4} T_e) + \log F({\rm He\ II}\ \lambda 1640)_{\rm obs} - \log F^*(1300)_{\rm obs} , \qquad (3)$$

which are analogous to equations (4) and (5) of Bohlin *et al.* In equations (2) and (3), $F({\rm H}\beta)_{\rm obs}$ and $F({\rm He\ II}\ \lambda 1640)_{\rm obs}$ are the observed fluxes (ergs cm^{-2} s^{-1}) of the nebular Hβ and He II λ1640 lines, respectively; $F^*(1300)_{\rm obs}$ is the observed stellar flux in ergs cm^{-2} s^{-1} Å^{-1}; and $\eta_{\rm H^0}$ and $\eta_{\rm He^+}$ are the fractions of the stellar photons shortward of 912 Å and 228 Å, respectively, which are absorbed in the nebula. T_e is the electron temperature of the nebula, and c_β is the logarithmic extinction at Hβ, related to the color excess by $c_\beta = 1.48E(B-V)$. The interstellar extinction curve of Savage and Mathis (1979) has been used. The choice of λ_* equal to 1300 Å is motivated by two reasons. First, good measurements of the flux at 1300 Å are possible in planetary nebulae with the *IUE* satellite, while B and V magnitudes of central stars are uncertain because of heavy contamination by nebular continuum and lines. Second, the correction for the contribution of the nebular continuum in the observed UV and optical range is smallest around 1300 Å (see Heap and Augensen 1987). The disadvantage of the comparison of the nebular Hβ flux with the stellar 1300 Å flux, which implies a differential extinction over a long wavelength range, is negligible in our two stars because they have quite a low reddening.

Using expressions (2) and (3), one can obtain $Q(912, 1300)$ and $Q(228, 1300)$ from the observations if the quantities on the right-hand side of equations (2) and (3) are known and if $\eta_{\rm H^0}$ and $\eta_{\rm He^+}$ can be inferred. By comparing these "observational" Q-values with the theoretical ones, one derives the star's parameters.

We collect in Table 2 properties of NGC 6543 and NGC 6826 which are needed in equations (2) and (3). The designation of the quantities is self-explanatory, except for f_{IUE}, which is the fraction of the nebula (assumed homogeneous) estimated to enter into the *IUE* large-aperature slot ($\sim 10'' \times 20''$ oval). The adopted quantities are taken from the literature except for most of the UV properties, which are from the present paper (see below).

Using the values in Table 2, we obtain the observed Q-values

© American Astronomical Society • Provided by the NASA Astrophysics Data System

1989ApJ...337..382P

TABLE 2

PROPERTIES OF NGC 6543 AND NGC 6826[a]

Property	NGC 6543	Sources	NGC 6826	Sources
		Nebula		
c_β	0.12 0.08–0.14[b]	1, 2, 3, 4, 5	0.03 0.02–0.04[b]	1, 2, 3
$F(\mathrm{H}\beta)$	2.5(−10)	6, 7, 8, 9, 10, 11, 12	1.2(−10)	6, 7, 8, 9, 12, 18, 19
$F(\mathrm{He}^+\ \lambda 1640)$[c]	<1.1–(11)	13	<3.9(−12):	13
T_e (K)	8100	14, 15	11200	20, 21, 22
N_e (cm^{-3})	6000	14, 15	4100	20
		Central Stars		
Spectrum	Of–W-R	16	O4f	16
V (mag)	10.93	17	10.48	23
$F(1300)$[d]	1.06(−11) 1.01(−11)	13 13	1.08(−11) 1.07(−11)	13 13
$F(1640)$[d]	3.63(−12) 3.01(−12)	13 13	7.41(−12) 7.29(−12)	13 13
f_{IUE}	0.8	13	0.42	24

NOTE.—Parentheses enclose powers of factor 10.

[a] Line fluxes are in ergs cm^{-2} s^{-1}. Continuum fluxes are in ergs cm^{-2} s^{-1} Å^{-1}.

[b] Estimated error interval.

[c] The observed values are indicated as upper limits, because most of the line is of stellar origin (see (text).

[d] The first number is the observed value. The second one is the first after substraction of the nebular contribution (see text).

REFERENCES.—(1) Pottasch *et al.* 1977 (*ANS* satellite, 2200 Å bump); (2) Kaler 1976 (radio/Hα); (3) Kaler 1983 (Balmer decrement); (4) Kaler 1986 (Balmer decrement); (5) Bianchi, Cerrato, and Grewing 1986 (2200 Å bump); (6) Razmadze 1958; (7) Capriotti and Daub 1960; (8) Liller 1955; (9) Liller and Aller 1954; (10) Vorontsov-Velyaminov 1965*a*; (11) Tamura 1970; (12) Kaler 1978*b*; (13) present paper; (14) Aller and Czyzak 1979; (15) Barker 1983; (16) Heap and Augensen 1987; (17) Kaler 1981*b*; (18) Vorontsov-Velyaminov 1965*b*; (19) Razmadze 1956; (20) Aller and Czyzak 1983; (21) French 1981; (22) O'Dell 1963; (23) C.-Y. Shao and W. Liller 1973, unpublished; (24) Coleman, Reay, and Worsik 1975.

given in Table 3. By comparison with the theoretical values of Q calculated from the LTE model atmospheres with metals of Hummer and Mihalas (1970), we evaluate the corresponding values of T_Z, also shown in Table 3.

The T_Z values in column (3) of Table 3, i.e., those coming from $Q(912, 1300)$, are lower limits, while those in column (5), which come from $Q(228, 1300)$, are upper limits. The first follows from the fact that it is difficult to be sure about the completeness of the absorption of the 228 Å $< \lambda <$ 912 Å photons. Therefore η_{H^0} may be less than unity, which causes the corresponding T_Z to be a lower limit.

The absorption of the $\lambda <$ 228 Å photons in the nebulae is usually complete (unless geometrical holes are present). The η_{He^+} should be 1.0 for this reason. However, part of the photons below $\lambda = 228$ Å might be absorbed in the wind, which would cause the corresponding T_Z to be a lower limit. At present we accept the simplification that the winds are optically thin at $\lambda <$ 228 Å and also for 228 Å $< \lambda <$ 912 Å. On the other hand, in our two stars the nebular emission in the He II λ1640 line is only an upper limit, and this causes T_Z in column (5) to be an upper limit.

TABLE 3

OBSERVED $Q(\lambda_0, 1300)$ AND CORRESPONDING T_Z

Central Star (1)	$\eta_{\mathrm{H}^0}\,Q(912, 1300)$ (2)	T_Z (K) (3)	$\eta_{\mathrm{He}^0}Q(228, 1300)$ (4)	T_Z (K) (5)
NGC 6543....	0.40	≥47,000	1.1×10^{-3}	≤70,000
NGC 6826....	0.25	≥42,000	1.3×10^{-3}	≤60,000

ii) *IUE Observations*

The above information on T_Z can be complemented by matching the theoretical stellar fluxes to the observed stellar continuum. In principle this is best done over a long wavelength range. However, in our hot stars the optical range adds little information, being on the Rayleigh-Jeans tail. Moreover, in this range there is a severe contamination by the nebular radiation. It is then appropriate to restrict consideration to the UV range observed with *IUE*.

NGC 6543.—Despite the several spectra available in low resolution, it is not simple to obtain an absolutely calibrated spectrum of the central star from 1200 to 3200 Å, as has been recognized by Bianchi, Cerrato, and Grewing (1986, hereafter BCG). An absolute spectrum in the 1200–2000 Å interval has been published by Castor, Lutz, and Seaton (1981, hereafter CLS). (Image SWP 1711, SA, 5 minute exposure.)

The absolute flux is calculated assuming a transmission factor of 0.5 because the spectrum was taken with the small aperture (circular 3″ diameter). From Figure 1 of CLS one reads $F^*(1300) = 6.9 \times 10^{-12}$ ergs cm^{-2} s^{-1} Å^{-1}. This is close to the value published by Heap and Augensen (1987) of 7.7×10^{-12}, using the prelaunch ITF on the image SWP 1328. Both numbers differ from the value of 4.9×10^{-13} that can be read from the observed spectrum (1200–3200 Å) published by BCG in their Figure 1. This spectrum results from a combination of various SA and LA images, where SA and LA refer

© American Astronomical Society • Provided by the NASA Astrophysics Data System

1989ApJ...337..382P

to small- and large-aperture observations. Since, moreover, the ratio of fluxes in the continuum $F(1300)/F(1640)$ of the BCG spectrum is rather different from that of CLS, we have decided to look again at all the low-resolution images of NGC 6543 in the *IUE* archive. The only images in low resolution, among those available up to now, which can be used for studying the central star, i.e., free from saturation in the continuum and not offset from the central star are SWP 1711 SA, 1897 LA, 8952 SA, 20123 SA, and LWR 1761 LA, 2925 LA, and 7705 SA. The observed absolute fluxes at 1300 and 1640 Å, in the continuum, are taken from the only LA image available at the shortest wavelengths: SWP 1897. They are reported in Table 2. These values have to be corrected for the atomic continuum emitted by the nebula and for the stellar light scattered by dust particles in the nebula. We neglect this last contribution because the gas-to-dust ratio is usually much higher in planetary nebulae than in H II regions, and we know that in the Orion Nebula the dust-scattered light falling within the large aperture of *IUE* adds little to the luminosity of the illuminating star θ^1 Ori C (falling within the same aperture) (Perinotto and Patriarchi 1980). For calculating the atomic nebular contribution to the observed flux, we have used the theory of Brown and Mathews (1970), with the electron temperature and density, the flux at Hβ, and the parameter f_{IUE} from Table 2 and the helium abundances from Table 1.

The fluxes corrected for atomic nebular contribution are also shown in Table 2. The correction is small, particularly at 1300 Å. The obtained stellar flux at 1300 Å (1.01×10^{-11} ergs cm^{-2} s^{-1} Å^{-1}) is close to the value determined from CLS and Heap and Augensen (1987), and also to the values 1.09×10^{-11} and 7.28×10^{-12} ergs cm^{-2} s^{-1} which come from the images SWP 8952 SA and SWP 20123 SA (after allowing for a transmission factor of the small aperture of 0.5).

To measure the flux in the emission line He II λ1640, we have used the SWP 1897 LA image, obtaining 1.05×10^{-11} (ergs cm^{-2} s^{-1}). We avoided correcting for the *IUE* aperture, because the nebular size in the optical (essentially identical to the one in Hβ) is small relative to the large aperture ($f_{IUE} = 0.8$). It is also true that the nebular emission by He II lines is likely to fall all within the large *IUE* aperture, because there is evidence that the He II emission is detected only in regions close to the star (Boeshaar, Czyzak, and Aller 1974).

The problem of the origin of the He II line emission, whether it is nebular or stellar, has been discussed by CLS, who on the basis of optical spectra and their small-aperture *IUE* spectrum conclude that not more than a third of the observed He$^+$ line emission is formed in the nebula. With more UV spectra we can confirm their point: the stellar contribution is dominant. In fact, from their SA spectrum, CLS obtain a flux of the He II λ1640 line of 1.19×10^{-11} ergs cm^{-2} s^{-1}, and we find 1.24×10^{-11} and 1.22×10^{-11} ergs cm^{-2} s^{-1} from SWP 8952 SA and SWP 20123 SA, respectively. These values are obtained always allowing for a transmission correction factor of 0.5. The comparison with the above value of 1.05×10^{-11} ergs cm^{-2} s^{-1} from the large aperture already tells us that the emission is substantially stellar. Moreover, from a high-resolution spectrum (SWP 3323 LA) we measure a line width at the level of the continuum of 4.5 Å, much more than that of nebular forbidden lines in the same spectrum. No absorption component is seen. We then infer that practically all the energy is formed very near to the star. We recognize, however, the possibility that about 10% of the energy is formed in the nebula. This amount is used to obtain the upper limit of 70,000 K in Table 3, via the calculation of the "observed" $Q(228)$ (see above).

The whole (1200–3000 Å) stellar spectrum, shown in Figure 1, is derived by combining SWP 8952 SA with LWR 7705 SA, which match each other in the overlapping region of wavelengths. This spectrum will be used later on for comparison of the continuum with model atmosphere calculations.

NGC 6826.—The observed UV fluxes given in Table 2 have been derived from the images SWP 16328 LA and LWR 12580. Using the same procedure as for NGC 6543, the absolute fluxes in the continuum 1300 and 1640 Å have been corrected for the nebular contribution. The observed and the corrected fluxes are given in Table 2. The value at 1300 Å is close to that given by Heap and Augensen (1987) of 7.9×10^{-12} ergs cm^{-2} s^{-1} Å^{-1} using the image SWP 1140 with the prelaunch ITF. There is some evidence of an emission line at 1640 Å. We measure it to be 3.9×10^{-12} ergs cm^{-2} s^{-1} from the image SWP 16328 LA and 3.3×10^{-12} ergs cm^{-2} s^{-1} from SWP 16328 SA. The high-resolution spectrum SWP 20896 LA shows an emission not quite prominent around 1640 Å, whose width at the level of the continuum is about 2.5 Å. This is much more than the width of the forbidden nebular lines seen in the same spectrum. So we infer that no more than 10% of the line can be of nebular origin. Correspondingly, we find the Zanstra temperature upper limit of 60,000 K quoted in Table 3.

The whole (1200–3200 Å) spectrum (SWP 16328 SA, LWR 12580 SA), shown in Figure 2, will be used later on for fitting with theoretical fluxes from model atmospheres.

iii) *Fit of the UV Stellar Continuum with Theoretical Fluxes*

NGC 6543.—The whole spectrum has been normalized to 1800 Å and corrected for reddening using c_β given in Table 2. The spectrum is shown in Figure 1, together with theoretical fluxes from the model atmospheres by Hummer and Mihalas (1970) with $T_{\rm eff} = 40{,}000$ K, $\log g = 4.5$ and $T_{\rm eff} = 100{,}000$ K, $\log g = 6.5$. We emphasize that in this spectral range the fluxes are rather insensitive to the gravity. In Figure 1 error bars at 1300, 2400, and 2900 Å are shown. These represent a combination of the reddening error (according to the uncertainty in reddening shown in Table 2) and of the internal error of $\pm 3\%$, i.e., the statistical error of *IUE* low-resolution spectra (Bohlin *et al.* 1980). Note that the error is zero at the normalization wavelength 1800 Å.

The observed fluxes, longward of 1800 Å, are not easily fitted with a specific model. Giving more weight to the fluxes longward of 2500 Å and shortward of 1800 Å, we feel that a model atmosphere with $T_{\rm eff} = 60{,}000$ K might represent the best choice. However, we recognize the uncertainty of this value.

NGC 6826.—The whole observed spectrum corrected for reddening with c_β from Table 2 and normalized to 1800 Å is compared in Figure 2 with fluxes from theoretical models. Error bars are shown as illustrated above for NGC 6543. A good fit is obtained here with models of Hummer and Mihalas (1970) around $T_{\rm eff} = 40{,}000$ K.

iv) *Conclusions on $T_{\rm eff}$*

By combining the information on the temperature obtained with the Zanstra method with those from the UV stellar continuum, we infer for the central stars of NGC 6543 and NGC 6826, $T_{\rm eff} = (60 \pm 10) \times 10^3$ K and $T_{\rm eff} = (45 \pm 10) \times 10^3$ K, respectively.

c) *Stellar Radius*

The stellar radius has been estimated in two ways: from evolutionary tracks and from the relation between the terminal velocity of the wind, v_∞ and the escape velocity $v_{\rm esc}$.

The evolutionary tracks for post–AGB stars in the (log g,

© American Astronomical Society • Provided by the NASA Astrophysics Data System

1989ApJ...337..382P

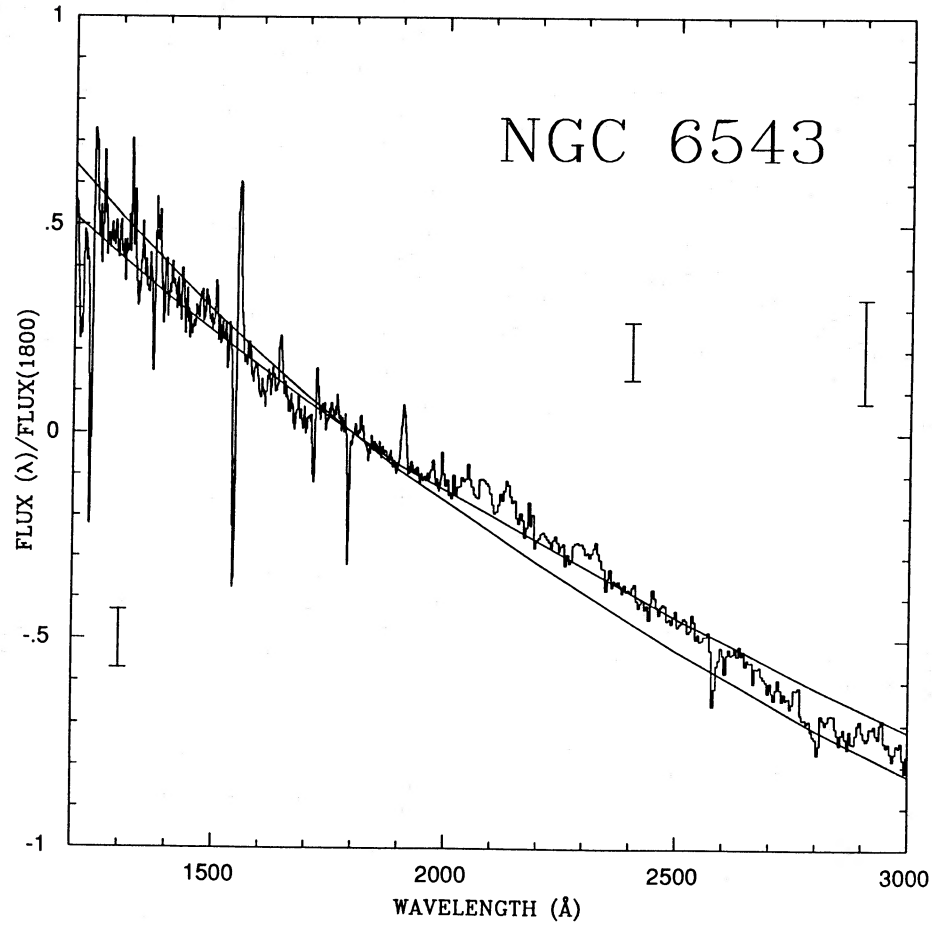

FIG. 1.—*IUE* low-resolution spectra of NGC 6543, dereddened and normalized to1800 Å, are compared with model atmospheres by Hummer and Mihalas (1970, series 200). The solid line higher at 1300 Å is the model with $T_{\rm eff} = 100{,}000$ K, log $g = 6.5$; the one smaller at 1300 Å is the model with $T_{\rm eff} = 40{,}000$ K, log $g = 4.5$. Error bars refer to extreme uncertainties of the observational data (see text).

log $T_{\rm eff}$)-diagram, as presented by Mendez *et al.* (1988), were adopted. Since most central stars have masses of about 0.6 $M_\odot$ (cf. Koester, Schulz, and Weidemann 1979; Heap and Augensen 1987), the values of log g which are derived from the (log g, log $T_{\rm eff}$)-diagram can be converted into radius. Using the temperatures of 60,000 and 45,000 K for NGC 6543 and NGC 6826, we find radii of $R_*/R_\odot = 0.20$ and 1.45, respectively, for the two stars.

The terminal velocity of the winds of Population I OB stars with $T_{\rm eff} > 3 \times 10^4$ K is related to the escape velocity at the photosphere by means of $v_\infty = (3 \pm 0.5)v_{\rm esc}$ (Abbott 1982). Using data from CP, we have seen that a similar relation also holds, with some scatter, for the central stars of planetary nebulae. Using the terminal velocities $v_\infty = 1900$ and 1750 km s^{-1} for NGC 6543 and NGC 6826 (see § III), and again assuming a mass of 0.6 $M_\odot$ for both stars, we estimate radii of $R_*/R_\odot = 0.57$ and 0.67, respectively, for the two stars. These values are lower than those derived from the evolution tracks.

Combining the two estimates and taking into account the scatter in the v_∞-$v_{\rm esc}$ relation, we adopt the following values for the radius: $R_*/R_\odot = 0.70^{+0.30}_{-0.10}$ for NGC 6543, and $1.45^{+0.64}_{-0.60}$ for NGC 6826. Correspondingly, the luminosities of the two stars are log $(L/L_\odot) = 3.75^{+0.59}_{-0.45}$ and $3.88^{0.67}_{-0.90}$. From the atmospheric models and the observed stellar flux at 1300 Å, we deduce for the ratio of the stellar radius to the distance of the star $R_*/d = 1.10 \times 10^{-11}$ and $R_*/d = 1.09 \times 10^{-11}$ for the two stars, which results in distances of 1440 and 2990 pc for NGC 6543 and NGC 6826, respectively. The parameters are summarized in Table. 4.

III. ANALYSIS OF THE STELLAR WINDS

a) Observations

NGC 6543.—The central star of this planetary nebula has been shown to exhibit P Cygni profiles in various UV lines of heavy ions by CLS, who have studied in detail the properties of the wind from a low-resolution *IUE* spectrum. The star has been studied subsequently in high resolution by BCG. These authors used the escape probability method in the Sobolev approximation to match the moment of the flux distribution or the line profiles, respectively.

Since we have developed a more complete method for the

TABLE 4

PARAMETERS OF PNCSs

Object (NGC)	$T_{\rm eff}$ (10^3 K)	$R_*/R_\odot$	log $(L/L_\odot)$	d (pc) Present Paper	d (pc) Daub 1982
6543.....	60 ± 10	$0.70^{+0.31}_{-0.10}$	$3.75^{+0.59}_{-0.45}$	1440	640
6826.....	45 ± 10	$1.45^{+0.67}_{-0.90}$	$3.88^{+0.67}_{-0.90}$	2990	1080

© American Astronomical Society • Provided by the NASA Astrophysics Data System

1989ApJ...337..382P

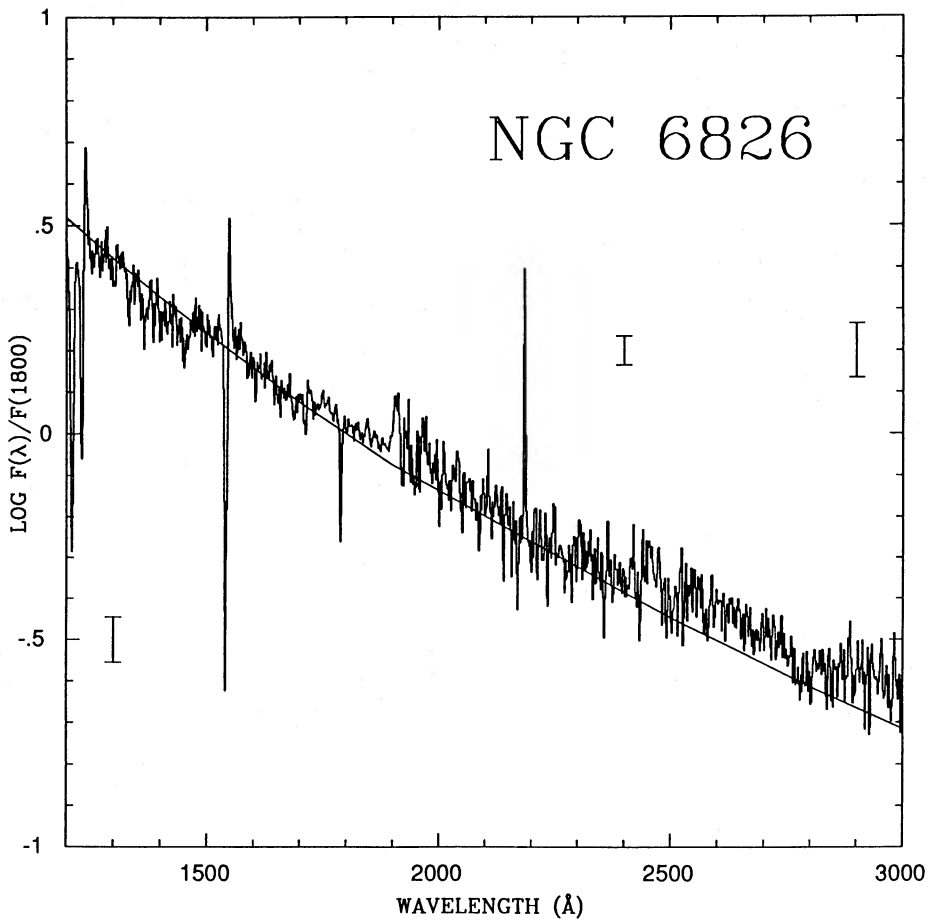

FIG. 2.—Same as Fig. 1, but for NGC 6826. The solid line is the Hummer and Mihalas (1970, series 200) model atmosphere with $T_{\rm eff} = 40{,}000$, $\log g = 4.5$.

analysis of the profiles, and also because of the problems with the best assessment of the stellar parameters, it is interesting to study again the wind of this star.

The high-resolution *IUE* image SWP 3323 has been used. The edge velocities from the various lines have been determined by checking the wavelength scale with interstellar absorption lines and the geocoronal Lyα line. The resulting velocity is similar for the N v λ1240 and C IV λ1549 doublets and is equal to 1900 ± 100 km s^{-1}. This is identical to the edge velocity found by BCG and is adopted as the terminal velocity v_∞ of the wind. The other lines exhibit smaller edge velocities. These are given in Table 5, as $w_1 = v_{\rm edge}/v_\infty$.

NGC 6826.—This object was observed in the commissioning phase of the *IUE* satellite and exhibits strong P Cygni lines in several UV lines (Heap *et al.* 1978). Later on it has been studied at low resolution by CP and with high-resolution spectra by Bombeck, Koppen, and Bastian (1986) and by Hutsemékers and Surdej (1987).

We have used the high-resolution *IUE* image SWP 20869. Clear P Cygni profiles are exhibited by the same lines as in NGC 6543, except for the Si IV doublet, i.e., by lines of the N v, C IV, O IV, O v, and N IV ions. The Si IV resonance lines at $\lambda\lambda$1393.73, 1402.73 appear in NGC 6826 as narrow, deep absorptions centered at the laboratory wavelengths. The Si IV doublet is therefore much weaker in the wind of NGC 6826 than in NGC 6543. This is the reverse of what would one expect, since the central star of NGC 6826 is cooler than the one of NGC 6543. A possible explanation is that the electron density is higher in the nucleus of NGC 6543, which in fact has Wolf-Rayet characteristics in the optical spectrum (see Table 2). Since at the temperatures of these stars Si v should be the dominant stage of silicon ionization, a higher density in NGC 6543 would produce a higher fraction of Si IV and therefore a

TABLE 5

PARAMETERS OF BEST FIT OF THEORETICAL PROFILES WITH OBSERVED PROFILES IN NGC 6543

Ion	λ (A)	w_1	β	α_2	T_B	W_G	ϵ'_0
N v	1238.82 1242.80	1.0	1.5	1	>100:	0.01	0.025
O IV.....	1338.60 1342.98 1343.51	0.76	1.5	2	1	0.01	10^{-5}
O v[a]	1371.29	0.79	1.5	2	3	0.01	10^{-5}
Si IV	1393.73 1402.73	0.73	1.5	1	0.5	0.01	10^{-5}
C IV	1548.20 1550.77	1.0	1.5	2	>100	0.01	0.05
N IV	1718.55	0.72	1.5	2	3	0.01	10^{-5}

[a] A photospheric line with $A_{\rm ph} = 0.3$ and $W_{\rm ph} = 0.2$ was assumed.

© American Astronomical Society • Provided by the NASA Astrophysics Data System

1989ApJ...337..382P

stronger feature in the wind of this star, despite its higher temperature. The edge velocity from the N V 1238.82 and C IV 1548.20 lines give similar results of around 1750 ± 100 km s^{-1}, which is adopted as the terminal velocity of the wind. This velocity is close to the 1900 km s^{-1} value adopted by CP from low-resolution spectra.

The other lines have smaller edge velocities. They are presented in Table 6 as $w_1 = v_{\rm edge}/v_\infty$.

b) *Profile Fitting with the SEI Method*

The SEI method for calculation of line profiles in stellar winds uses the Sobolev approximation to calculate the source function and solves exactly the transfer equation. It has been shown by LCP to give profiles very close to those calculated with the more powerful comoving-frame method by Hamann (1981), except for a small interval near the rest wavelength of the line.

With the SEI method, the wind's properties are determined by matching the observed profiles with theoretical ones. To compute the theoretical profiles, LCP choose the following parameterization of the velocity and opacity laws:

$$w(x) = w_0 + (1 - w_0)\left(1 - \frac{1}{x}\right)^{\beta}, \tag{4}$$

$$\tau(w) = \frac{T}{I}\left(\frac{w}{w_1}\right)^{\alpha_1}\left[1 - \left(\frac{w}{w_1}\right)^{1/\beta}\right]^{\alpha_2}, \tag{5}$$

$$I = w_1 \int_{w_0/w_1}^{1} y^{\alpha_1}(1 - y^{1/\beta})^{\alpha_2}\, dy\,, \tag{6}$$

where $x = r/R_*$ is the distance normalized to the stellar radius; $w = v(r)/v_\infty$, the velocity normalized to the terminal velocity; $w_1 = v_{\rm edge}/v_\infty$, so that $\tau(w) = 0$ for $w \geq w_1$; and T is the total optical depth in the line. This parameterization of $\tau(w)$ was chosen because it can represent any variation of the ionization in the wind with power-law dependence on velocity and distance (see LCP).

This implies the parameters w_0 and β for the velocity law, and α_1, α_2, T for the optical depth. We assume $w_0 = 0.01$, a frequently made assumption in the study of winds of hot stars, because it implies that the velocity of the base of the wind is approximately the thermal velocity. Also, we assume $\alpha_1 = 0$, since the observed profile show that $\alpha_1 \sim 0$. This reduces the number of parameters at the cost of the loss of some flexibility in the above parameterization, but it does not reduce the power of the method. The three remaining parameters are β, α_2, T.

To these one must add other parameters, which enter in the description of the source function: W_G, $A_{\rm ph}$, $W_{\rm ph}$, ϵ'_0, $(B_\nu/I_c)_0$, a_T. The first is a stochastic velocity, representative of local turbulence plus thermal motions. $A_{\rm ph}$ and $W_{\rm ph}$ are respectively the central depth and the FWHM of a Doppler profile assumed to represent the photospheric profile. The collisional term of the source function, normalized to the stellar continuum intensity, is $\epsilon' B_\nu/I_c$, where $\epsilon' = \epsilon'_0(w_0 x^{-2} w^{-1})$ and

$$B_\nu/I_c = (B_\nu/I_c)_0 \exp\left[-a_T(w - w_0)\right] \tag{7}$$

where B_ν is the Planck function and I_c the stellar continuum. At the base of the wind $x = 1$, $w = w_0$, which implies that $\epsilon' = \epsilon'_0$, and $(B_\nu/I_c) = (B_\nu/I_c)_0$. If the temperature of the wind is equal to the brightness temperature of the stellar continuum, the $(B_\nu/I_c)_0 = 1$. This is indeed assumed in this paper. The parameter $a_T > 0$ mimics a temperature decreasing outward, while $a_T < 0$ mimics an increasing temperature. We assume $a_T = 0$ and therefore a wind having approximately constant temperature.

The parameters we will deal with are therefore β, α_2, T, W_G, ϵ'_0, $A_{\rm ph}$, $W_{\rm ph}$. If the P Cygni lines are strong, one can ignore the photospheric profiles by setting $A_{\rm ph} = 0$ and $W_{\rm ph} = 0$. In the case of doublets, T_B and T_R represent the total optical depth of the bluer and redder component, respectively.

NGC 6543.—The generally used strategy to determine β, α_2, T, or their equivalent in other parameterizations, follows from the consideration that the emission component is very sensitive to the velocity law, therefore to β, and the absorption component to the opacity law, i.e., to α_2 and T. If one observes both optically thick and optically thin P Cygni lines in the star, then, since the first are saturated, the natural procedure is to use their emission to fix the value of β for the velocity law and then the optically thin lines to determine their optical depths. From the thick lines one can get only a lower limit to their optical depth.

This strategy may work in some stars, but it clearly fails in the case of the central star of NGC 6543. After several tests, we conclude that it is impossible to fit both the strong and the faint P Cygni lines with the same velocity law using only the parameters β, α_2, T. This is also evident in the work by BCG on this object (see their Fig. 3). They reproduce the profile of the N V doublet with $\beta = 2$, under the same parameterization of the velocity law that we use, but for C IV and O IV the fit is not very good.

Indeed, the SEI method includes even the role of the collisions in the source function through the parameters ϵ'_0, which proved to be important for the description of the wind in the central star of NGC 6543.

Optically thin lines are little affected by ϵ'_0, while the contrary is true for thick lines (see LCP). Therefore it is reasonable to start the analysis with a well-observed line that is as thin as possible. We chose the O IV triplet, which is seen at the *IUE* high resolution as a doublet. A theoretical profile with $\beta = 1.5$ ($\alpha_2 = 2$, $T = 1$) gives a good fit (Fig. 3). A theoretical profile with $\beta = 4$, on the other hand, still represents the absorption quite well but largely overestimates the emission components.

Let us now consider a well-observed thick line: the C IV doublet. With a negligible ϵ'_0 ($= 10^{-5}$) and $T_B = 100$, the emission is quite underestimated. To increase T_B does not help, because $T_B = 100$ already saturates the line. Instead an increase of ϵ'_0 to 0.05 produces a satisfactory fit (Fig. 4).

We present in Table 5 the best-fit parameters for the various P Cygni lines observed with the high-resolution *IUE* spectrum. They are the results of a long series of calculation of theoretical profiles for each line with the parameters varied as follows. For all lines, $\beta = (0.5, 1, 1.5, 2)$; $\alpha_2 = (1, 2, 3, 4)$; $\epsilon'_0 = (10^{-5}, 10^{-3},$

TABLE 6

PARAMETERS OF BEST FIT OF THEORETICAL PROFILES WITH OBSERVED PROFILES IN NGC 6826

Ion	w_1	β	α_2	T_B	W_G	ϵ'_0
N V	1.0	1.5	3	>100:	0.05	10^{-5}
O IV	0.50	1.5	4	1	0.05	10^{-5}
O V[a]	0.62	1.5	4	2	0.05	10^{-5}
C IV	1.0	1.5	3	>100	0.05	0.05
N IV	0.57	1.5	2	0.3	0.05	10^{-5}

[a] A photospheric line with $A_{\rm ph} = 0.4$ and $W_{\rm ph} = 0.5$ was assumed.

© American Astronomical Society • Provided by the NASA Astrophysics Data System

1989ApJ...337..382P

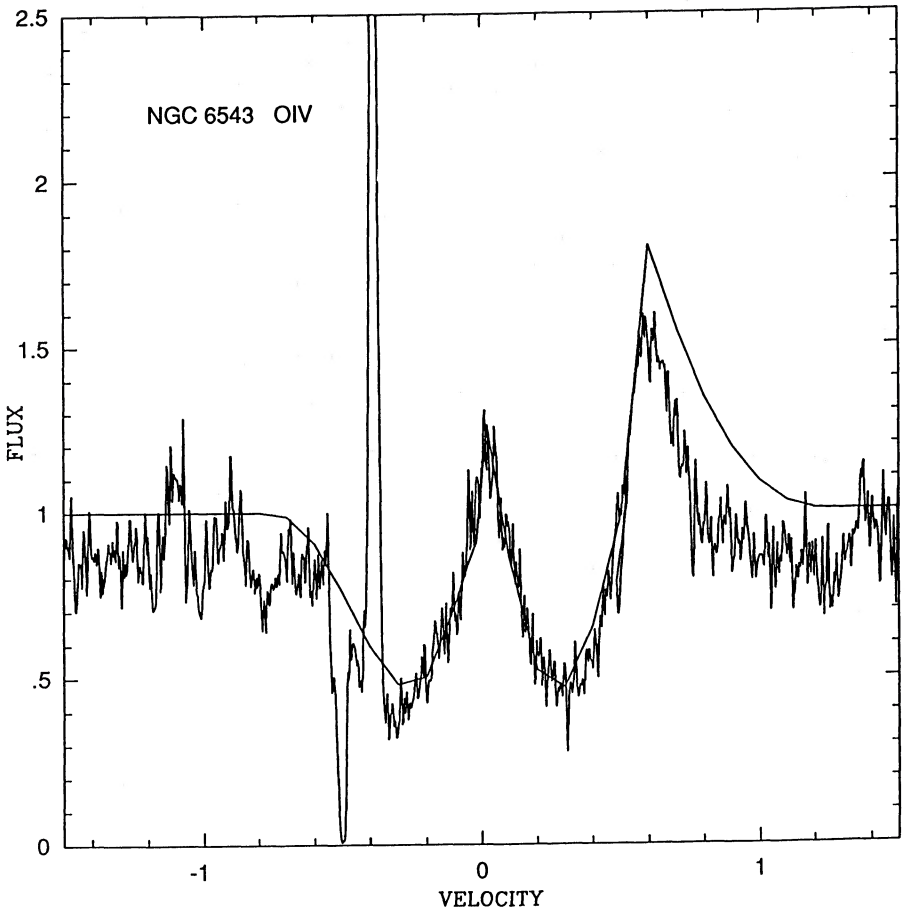

FIG. 3.—NGC 6543. Best fit of the observed *IUE* high-resolution profile of the O VI triplet with theoretical P Cygni profiles from the SEI method.

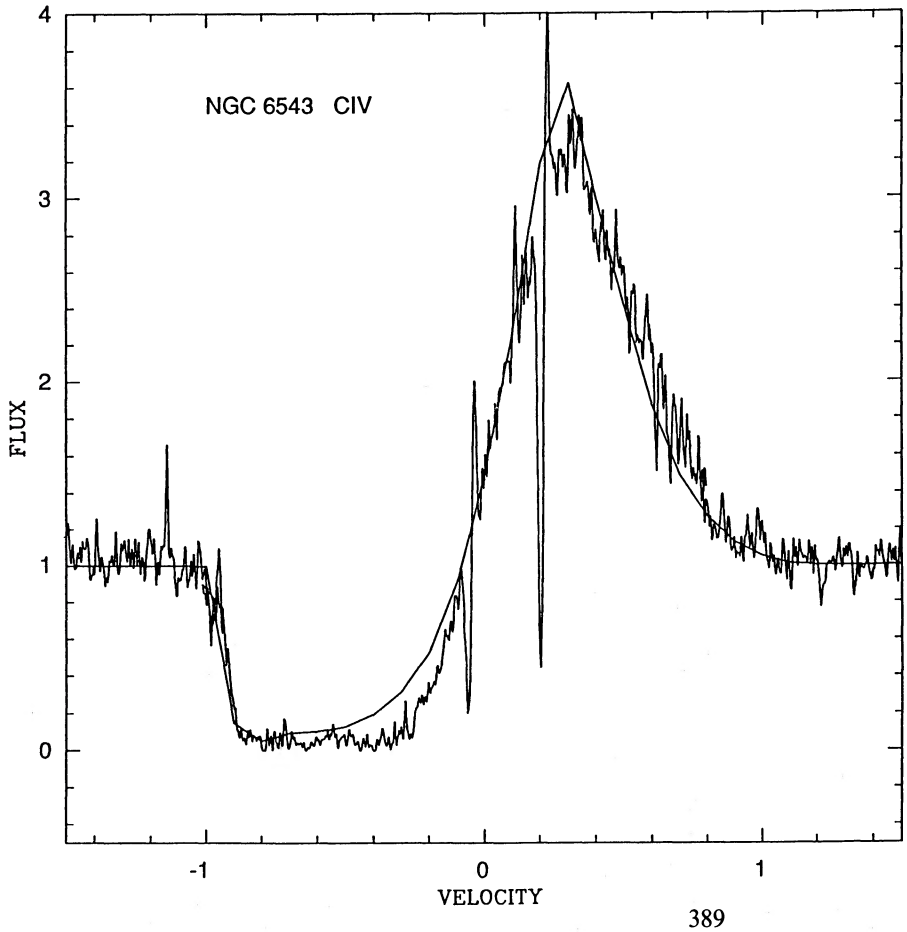

FIG. 4.—Same as Fig. 3, for the C IV doublet

© American Astronomical Society • Provided by the NASA Astrophysics Data System

1989ApJ...337..382P

10^{-2}, 10^{-1}), $W_G = (0.01, 0.05, 0.1)$. For thick lines $T = (10^2, 10^3)$, and for thin lines $T = (0.3, 0.5, 1, 2, 3, 4)$. That resulted in a grid of 384 profiles for thick lines and 1152 profiles for thin lines in each star (profiles for N IV and O V have been computed only once because the calculations are normalized to v_∞ and these lines are singlets). After selection of the best fit among the above basic profiles, individual adjustments have been made in specific lines. Figures 3–8 illustrate the quality of the final fits.

As anticipated above, the presence of an underlying photospheric profile was not necessary to reproduce the observed P Cygni profiles to the level we have accepted, except for the O V line. Indeed, an inspection of the spectrophotometric *IUE* atlas of Walborn, Nichols-Bohlin, and Panek (1985) shows that at wavelengths near the O V line there are various Fe V absorption lines which are rather prominent in the spectra of hot stars. In particular, the Fe V line λ1371.00 is very close to the O V line λ1371.29. We therefore felt justified in assuming that a photospheric absorption line of strength similar to those shown in the above-mentioned atlas underlies the formation of the observed O V line.

NGC 6826.—Using the same philosophy illustrated above for NGC 6543, we obtain the best-fit parameters shown in Table 6. The corresponding theoretical profiles are compared with the observations in Figures 9–13.

The agreement between the observed and the predicted profiles, shown in Figures 3–13, is reasonably good and considerably better than the fits made with Sobolev profiles (see, e.g., BCG). The main systematic difference between our theoretical best-fit profiles and the observed profiles is the underestimate of the absorption in the saturated lines at small velocities ($w < 0.2$). This may be due to additional absorption at low velocities, or to a larger stochastic velocities ($W_G > 0.05$) at low velocities (see LCP). For this reason we will exclude the part of the profile with $w < 0.2$ in the determination of the mass-loss rate.

c) *Mass-Loss Rates*

i) *Present Determination of $\dot{M}$*

With the parameterization adopted in the SEI method, the mass-loss rate of the wind is given by

$$\dot{M} q_i U_i = 1.23 \times 10^{-18} \frac{(R_*/R_\odot) v_\infty^2 (\mathrm{km\ s^{-1}})}{f \lambda_0 (\text{Å}) A_E} Z , \qquad (8)$$

with U_i and Z given by

$$U_i = W \frac{g_{i,l}}{g_{i,0}} \exp\left(-\frac{E_{l,g}}{kT_{\mathrm{rad}}}\right), \qquad (9)$$

$$Z = x^2 w \frac{dw}{dx} \frac{T}{I} \left(\frac{w}{w_1}\right)^{\alpha_1} \left[1 - \left(\frac{w}{w_1}\right)^{1/\beta}\right]^{\alpha_2}, \qquad (10)$$

where q_i is the ionization fraction of the ion; A_E is its elemental abundance relative to hydrogen; W is the geometrical dilution

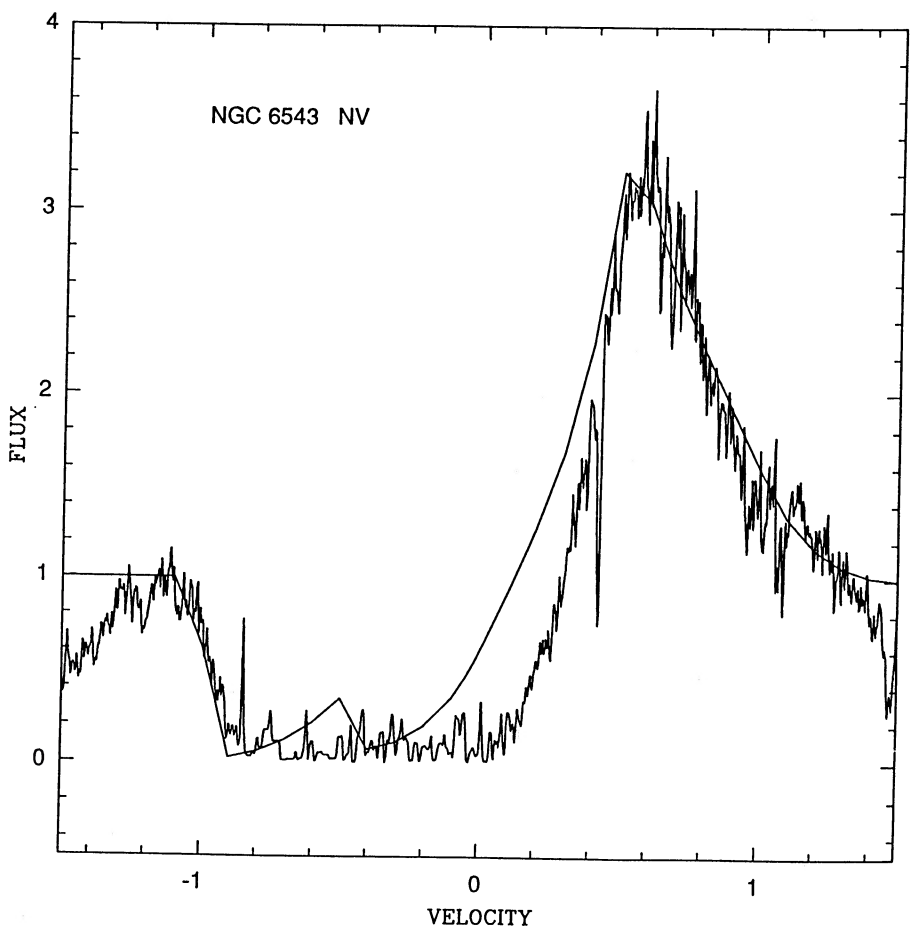

FIG. 5.—Same as Fig. 3, for the N V doublet

© American Astronomical Society • Provided by the NASA Astrophysics Data System

1989ApJ...337..382P

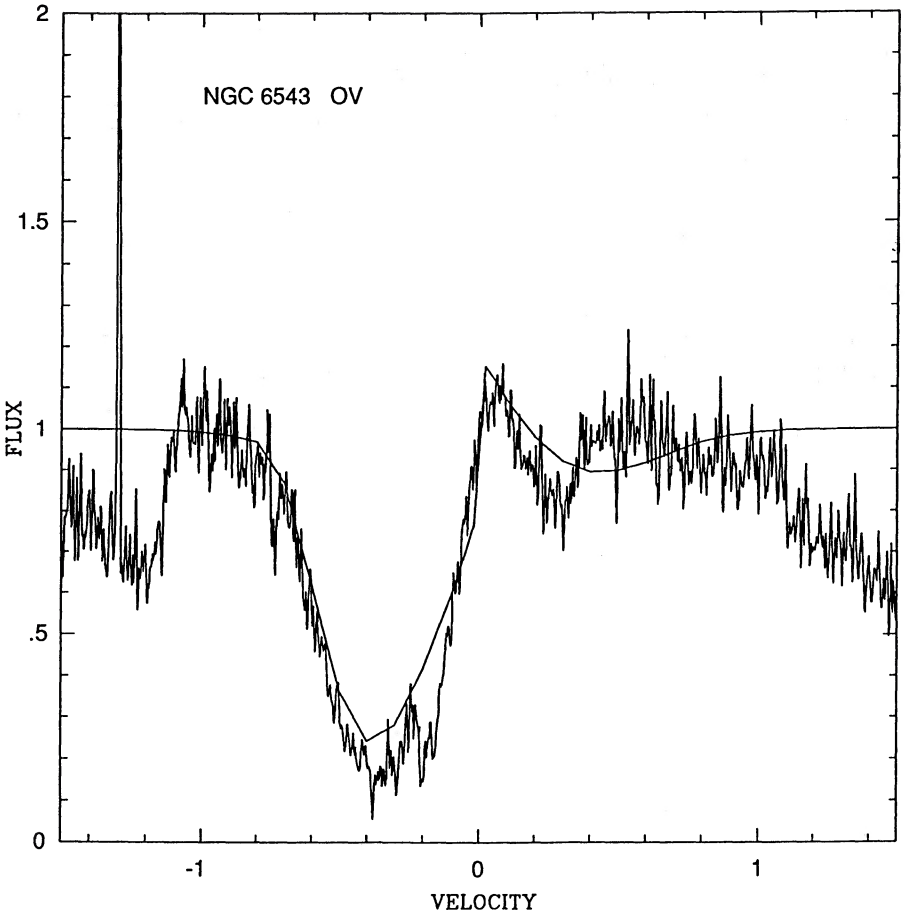

FIG. 6.—Same as Fig. 3, for the O V subordinate line

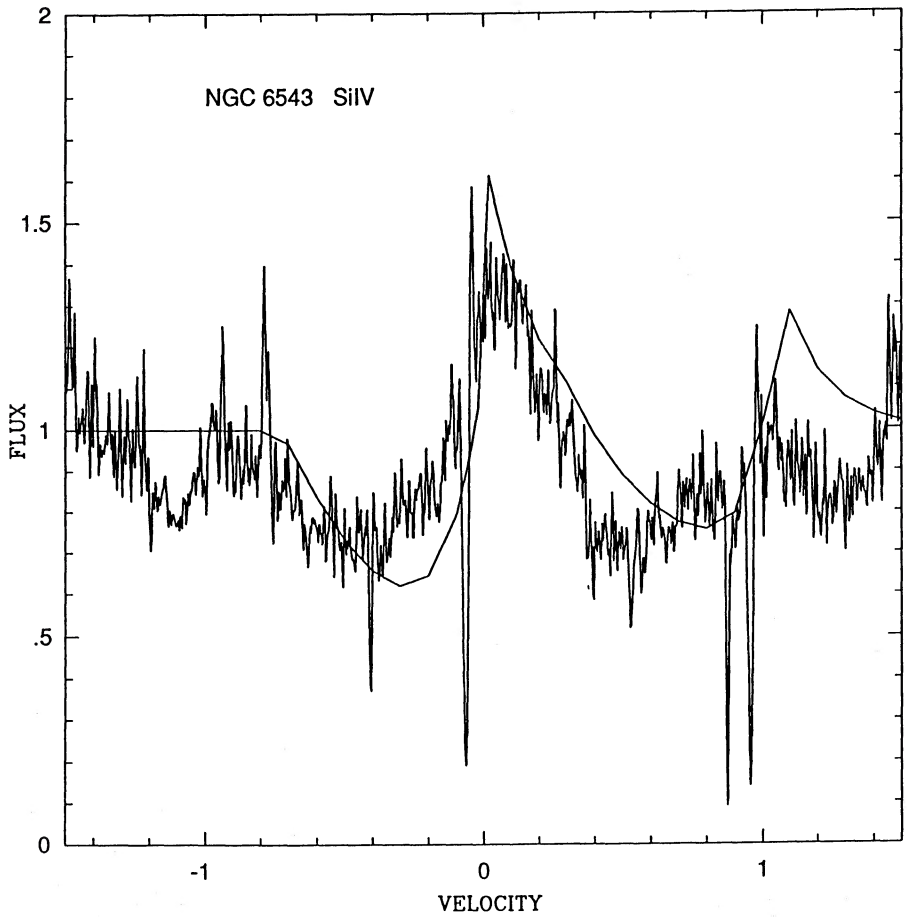

FIG. 7.—Same as Fig. 3, for the Si IV doublet

© American Astronomical Society • Provided by the NASA Astrophysics Data System

1989ApJ...337..382P

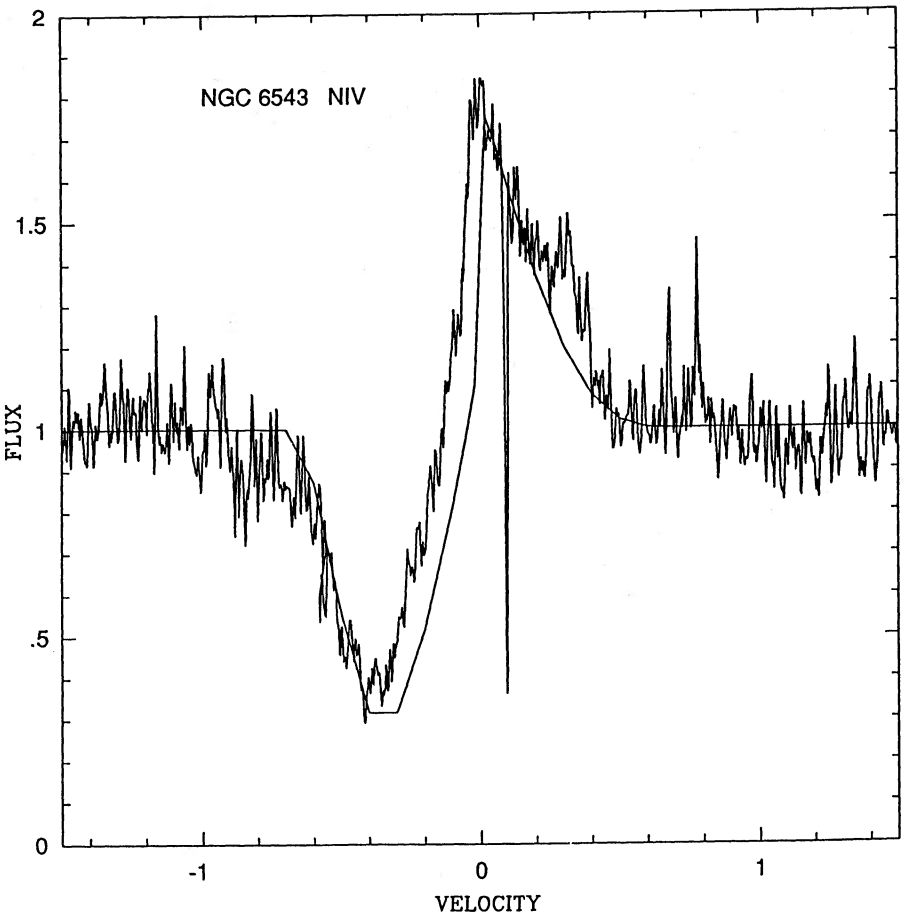

FIG. 8.—Same as Fig. 3, for the N IV subordinate line

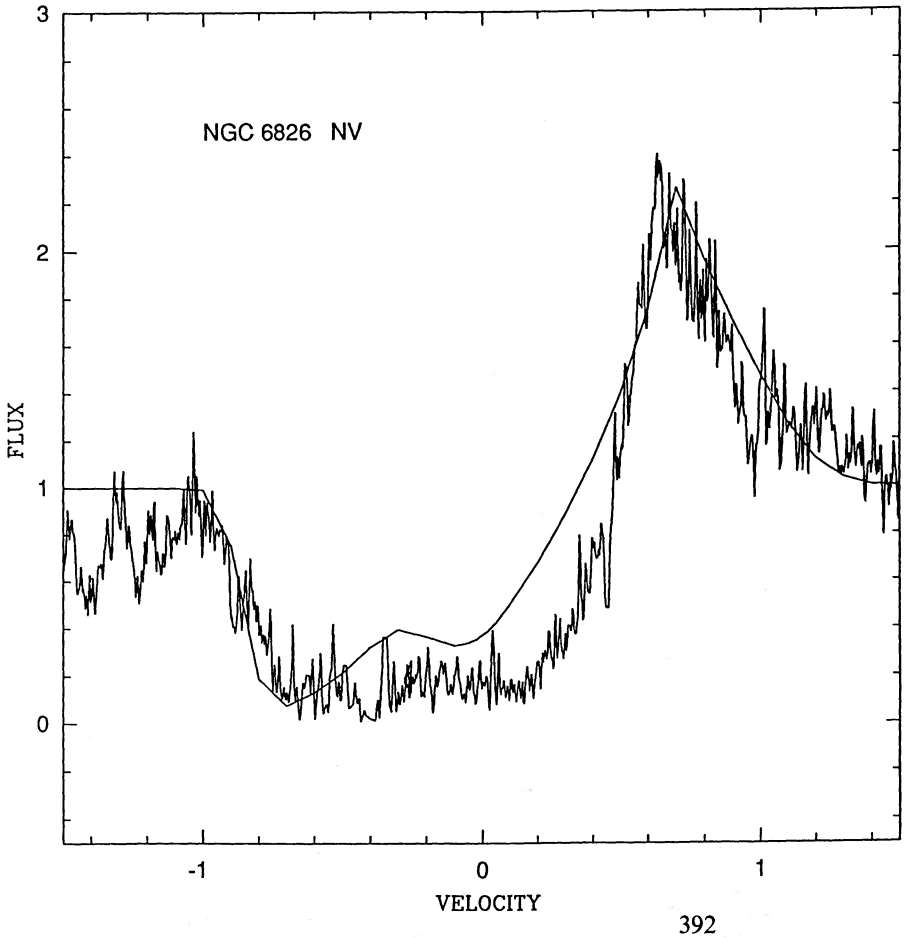

FIG. .—NGC 6826. Best fit of the observed *IUE* high-resolution profile of the N V doublet with theoretical P Cygni profiles from the SEI method.

© American Astronomical Society • Provided by the NASA Astrophysics Data System

1989ApJ...337..382P

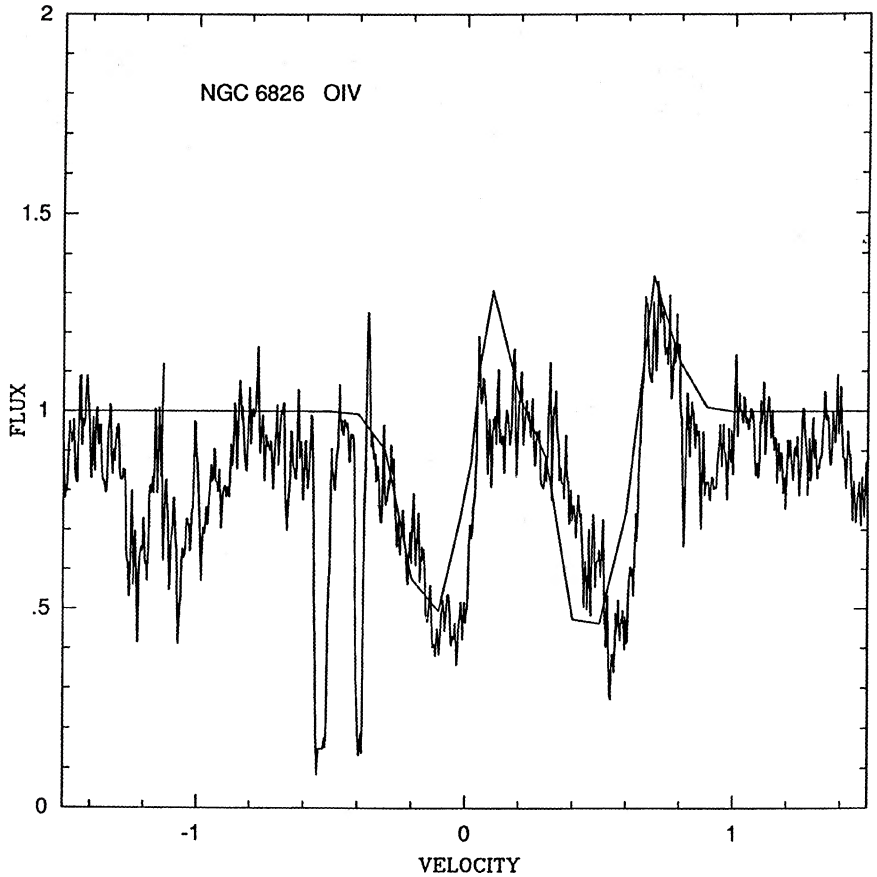

FIG. 10.—Same as Fig. 9, for the O IV triplet

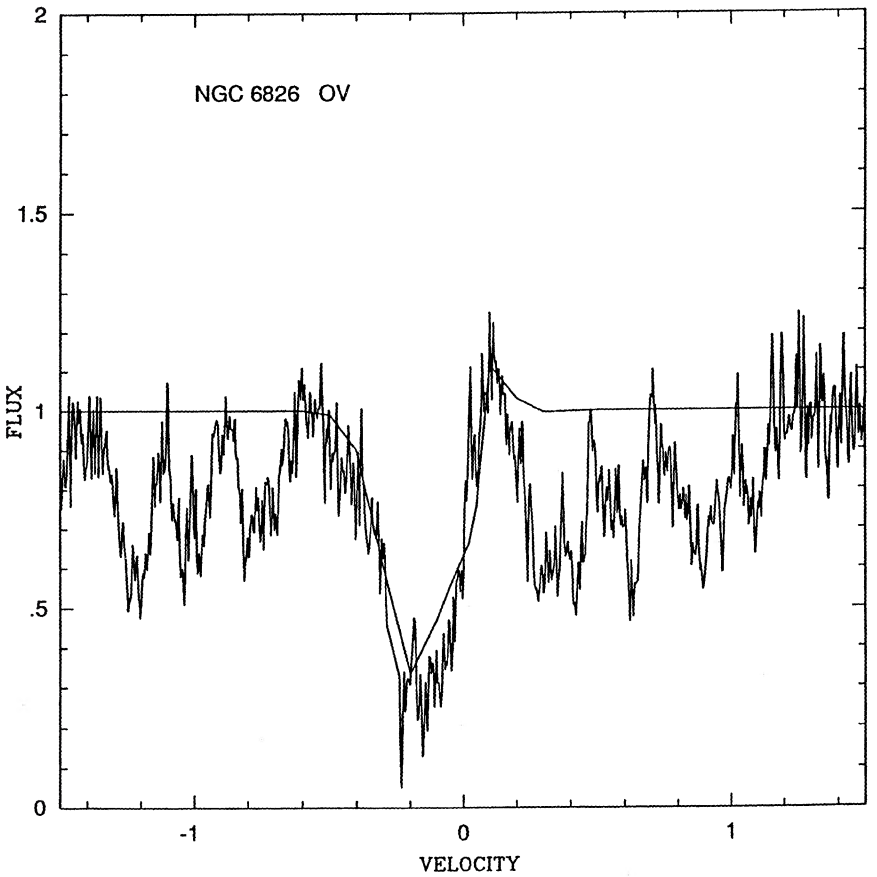

FIG. 11.—Same as Fig. 9, for the O V line

© American Astronomical Society • Provided by the NASA Astrophysics Data System

1989ApJ...337..382P

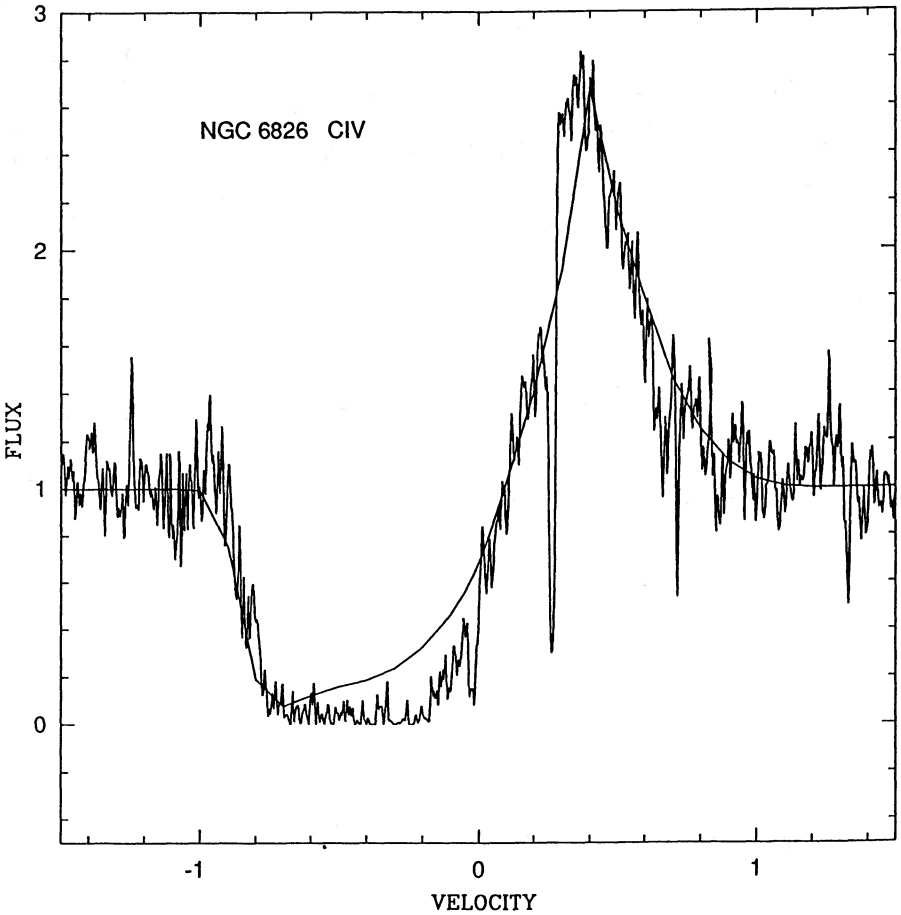

FIG. 12.—Same as Fig. 9, for the C IV doublet

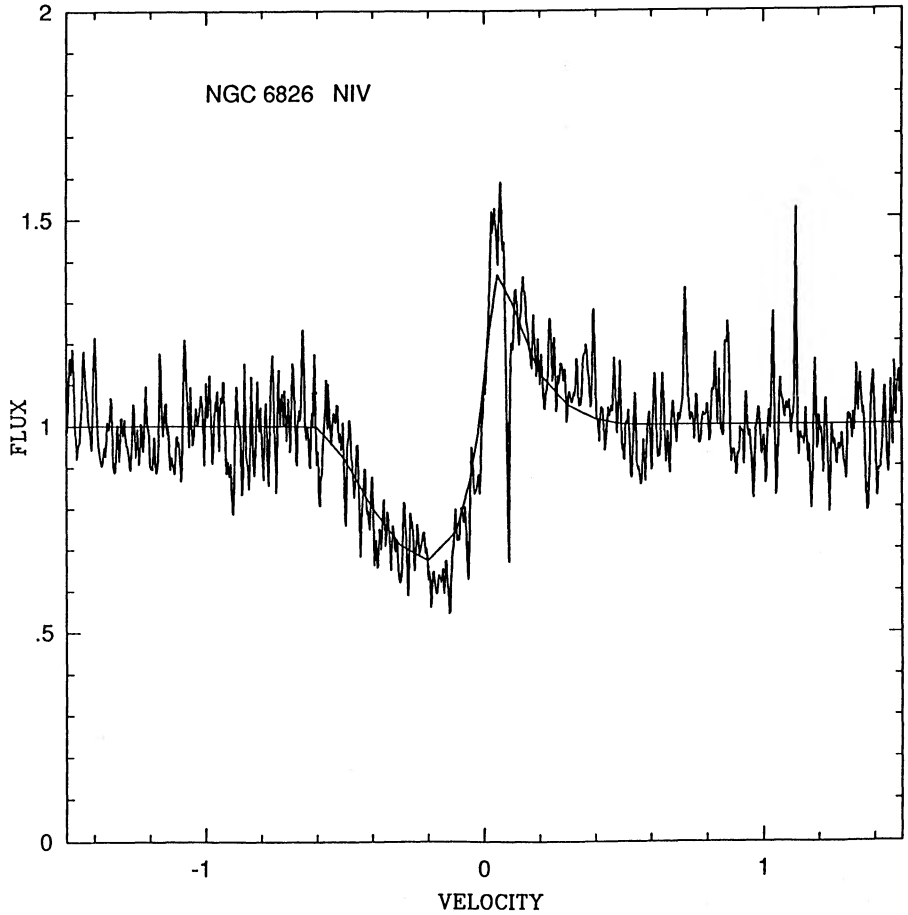

FIG. 13.—Same as Fig. 9, for the N IV line

© American Astronomical Society • Provided by the NASA Astrophysics Data System

1989ApJ...337..382P

TABLE 7

$\dot{M}\langle q\rangle$ ($M_\odot$ yr^{-1}) OF WINDS IN PNCSs

	NGC 6543		NGC 6826	
Ion (1)	$T = 60{,}000$ (2)	$T = 70{,}000$ $T = 50{,}000$ (3)	$T = 45{,}000$ (4)	$T = 55{,}000$ $T = 35{,}000$ (5)
C IV	≥5.6(−10)	4.8(−10) 8.0(−10)	≥2.8(−10)	4.2(−10) 1.1(−10)
N IV	1.0(−8)	5.5(−9) 2.7(−8)	9.3(−9)	1.6(−9) 4.5(−8)
N V	≥9.2(−9)	1.3(−8) 7.9(−9)	≥2.0(−8)	2.9(−8) 7.5(−9)
O IV	3.5(−8)	1.6(−8) 1.2(−7)	4.6(−8)	6.1(−9) 3.5(−7)
O V	5.4(−9)	2.7(−9) 1.7(−8)	6.3(−9)	9.4(−10) 3.9(−8)
Si IV	2.5(−11)	2.1(−10) 3.6(−11)	...	

NOTE.—Parentheses enclose powers of factor 10.

factor; f is the oscillator strength of the transition; $g_{i,0}$ and $g_{i,l}$ are the statistical weights of the ground level and of the lower level of the observed transition, respectively; $E_{l,g}$ is the energy of the lower level of the observed transition; $T_{\rm rad}$ is the radiation temperature at the wavelength whose energy is $E_{l,g}$. U_i is the excitation fraction of the observed ion; $U_i = 1$ for resonance lines. The constant in equation (8) is valid for a wind in which H and He are fully ionized and helium has an abundance by number of He/H = 0.10.

The lines which excite the lower levels of the observed transitions of the subordinate lines fall in the UV region between the H and the He^0 ionization limits. Our knowledge of $T_{\rm rad}$ remains here uncertain because even the very good atmospheric models of Hummer and Mihalas (1970) that we have used are incomplete. In particular, when a stellar wind is present, there is a backwarming effect toward the photosphere which enhances the radiation field significantly in the far-UV (Friend and Abbott 1986). This reduces the absorption edges at the ionization thresholds of the various ions, in particular of H and He, and causes the radiation to become closer to the blackbody behavior. Because of this uncertainty, we prefer in the following to assume simply $T_{\rm rad} = T_{\rm eff}$.

We derive $\dot{M}\langle q_i\rangle$ by integrating equation (8) between $w = 0.2$ and w_2, with $w_2 = 0.8$ for the saturated lines of N V and C IV and $w_2 = w_1$ for the other lines. Then $\langle q_i\rangle$ represents the fractional ionization averaged across the region of the wind where $0.2 < w < w_2$.

With the fitting parameters of Tables 5 and 6 and the fundamental stellar data from Table 4, we obtain $\dot{M}\langle q_i\rangle$ given in Table 7. The f-values from Lamers and Morton (1976) have been used. Columns (2) and (4) give $\dot{M}\langle q_i\rangle$ for the temperatures and corresponding radii adopted for the two central stars. Columns (3) and (5) show the changes when the temperatures (and correspondingly the radii) are varied according to the uncertainties quoted in Table 4.

A quite reasonable hypothesis for the ionization is to assume $q_{\rm O\,IV} + q_{\rm O\,V} = 1$ (cf. CLS). Then we obtain $\dot{M} = 4.0 \times 10^{-8}$ and 5.2×10^{-8} $M_\odot$ yr^{-1} for the central stars of NGC 6543 and NGC 6826, respectively. The accepted uncertainty in $T_{\rm rad}$ and in radius, taken as the dominant sources of error, gives for NGC 6543 and NGC 6826 $\dot{M} = (4.0^{+10}_{-2.1}) \times 10^{-8}$ and $\dot{M} = (5.2^{+34}_{-4.5}) \times 10^{-8}$ $M_\odot$ yr^{-1}.

This corresponds to an accuracy of a factor close to 3 in the first object. In the second object the accuracy is less.

ii) *Ionization Fractions*

Using the values of the mass-loss rates given above, we can derive the mean ionization fractions in the wind from the values of $\dot{M}\langle q\rangle$ in Table 7. We find approximately the same degree of ionization in both stars $\langle q_{\rm C\,IV}\rangle \geq 0.01$ in NGC 6543 and ≥0.005 in NGC 6826; $\langle q_{\rm N\,V}\rangle \geq 0.2$ in NGC 6543 and ≥0.4 in NGC 6826; $\langle q_{\rm N\,IV}\rangle \sim 0.2$, $\langle q_{\rm O\,IV}\rangle \sim 0.9$, $\langle q_{\rm O\,V}\rangle \sim 0.1$ in both stars; and $\langle q_{\rm Si\,IV}\rangle \sim 6 \times 10^{-4}$ in NGC 6543. These values are reasonable for winds of stars with $T \sim 5 \times 10^4$ K, in which C IV, N V, and O IV are the dominant ionization stages.

iii) *Comparison with Previous Determinations of $\dot{M}$*

We compare here our determinations of $\dot{M}$ with the previous ones of the same nature, i.e., direct empirical determinations. All determinations of this kind made so far of the mass-loss rate from the central stars of NGC 6543 and NGC 6826 are collected in Table 8. In each star the most extreme values of $\dot{M}$ differ by about a factor of 100. The determinations in Table 8 come from different methods, namely, (i) the escape probability method developed by Castor (1970), on which the widely used Castor and Lamers (1979) atlas of theoretical profiles is based; (ii) the first moment of the flux distribution method worked out by CLS, particularly suited for low-resolution *IUE* data; (iii) this same method modified to consider the effects of the optical thickness of subordinate lines (Surdej 1983); (iv) the SEI method of LCP; (v) a method similar to SEI, but less complete, used by Bombeck, Koppen, and Bastian (1986).

Method (ii) has been used on NGC 6543 by CLS, and on NGC 6826 by CP. Method (iii) has been used on both stars by Hutsemékers and Surdej (1987), all with low-resolution *IUE* data. The other determinations of $\dot{M}$ in Table 8 come from high-resolution *IUE* data with method (i) by Heap (1981) and

TABLE 8

MASS-LOSS RATES ($M_\odot$ yr^{-1}) FROM PNCSs

PN	This Paper	Other Papers
NGC 6543.....	4.0×10^{-8}	8.9×10^{-8},[a] 7.0×10^{-7},[b] 3.2×10^{-7},[c] 1.7×10^{-6} [d]
NGC 6826.....	5.2×10^{-8}	2.0×10^{-8},[e] 1.7×10^{-6},[f] 1.5×10^{-7} [d]

[a] Castor, Lutz, and Seaton 1981.
[b] Heap 1981.
[c] Bianchi, Cerrato, and Grewing 1986.
[d] Hutsemékers and Surdej 1987.
[e] Cerruti-Sola and Perinotto 1985.
[f] Bombeck, Koppen, and Bastian 1986.

© American Astronomical Society • Provided by the NASA Astrophysics Data System

1989ApJ...337..382P

BCG, with method (iv) in the present paper, and with method (v) by Hutsemékers and Surdej (1987).

In principle the determinations made with high-resolution *IUE* data should be more accurate, because all the information contained in the P Cygni profiles is used. We see, however, in Table 8 that very different $\dot{M}$ have been obtained by different authors using the same high-resolution data on the same object.

The differences then lie partly in the methods used to analyze the observations and partly in the different stellar parameters adopted by the various authors, including the assumptions relative to the ionization structure. Moreover, some authors use P Cygni lines different from those used by others.

It is evidently not simple to disentangle the various effects to clarify why each individual value appears as we see it. We only underline that both the method and the adopted stellar parameters may heavily influence the resulting $\dot{M}$.

For instance, in NGC 6543, the values of $\dot{M}$ found by CLS and by Hutsemékers and Surdej (1987) come from the same low-resolution observational quantities, under the same hypothesis for the ionization structure, but they differ by a factor of 20 in the mass-loss rate of NGC 6543. If we insert the R, T of the present paper instead of the corresponding numbers adopted by the authors, their $\dot{M}$ would become 1.2×10^{-8} and 9.1×10^{-8} $M_\odot$ yr^{-1}, respectively. The difference between these numbers is then due only to the different methods used for interpreting the same data.

This example illustrates the following: (1) the difference in $\dot{M}$ due only to the method may amount to 1 order of magnitude and (2) the difference in $\dot{M}$ because of the different stellar parameters adopted may also amount to 1 order of magnitude, because Hutsemékers and Surdej (1987) obtain 1.7×10^{-6}, while from their equations, by changing only the adopted stellar radius and temperature, we obtain for NGC 6543 $\dot{M} = 9.1 \times 10^{-8}$ $M_\odot$ yr^{-1}. The most critical stellar parameter is the radiation temperature at the wavelengths of the lines exciting the lower levels of the observed subordinate lines. This is because $T_{\rm rad}$ enters exponentially via the factor U_i (eq. [11]) in the mass-loss rate deduced from the subordinate lines. For example, an error of $T_{\rm rad}$ by +20% or −20%, at 60,000 K, would change the mass-loss rate by a factor of 0.5 or 2.8, respectively. We consider our determination of the mass-loss rates more reliable than previous estimates, for the following reasons. We have derived the basic parameters of the stars as accurately as possible from the existing data. We have used high-resolution *IUE* data which allow the deduction of the velocity and opacity laws appropriate for the two stars. When working with low-resolution *IUE* data, these laws have to be assumed (from studies of other stars). Actually the laws we have found are different from those adopted by the authors who have studied with low-resolution *IUE* data of NGC 6543

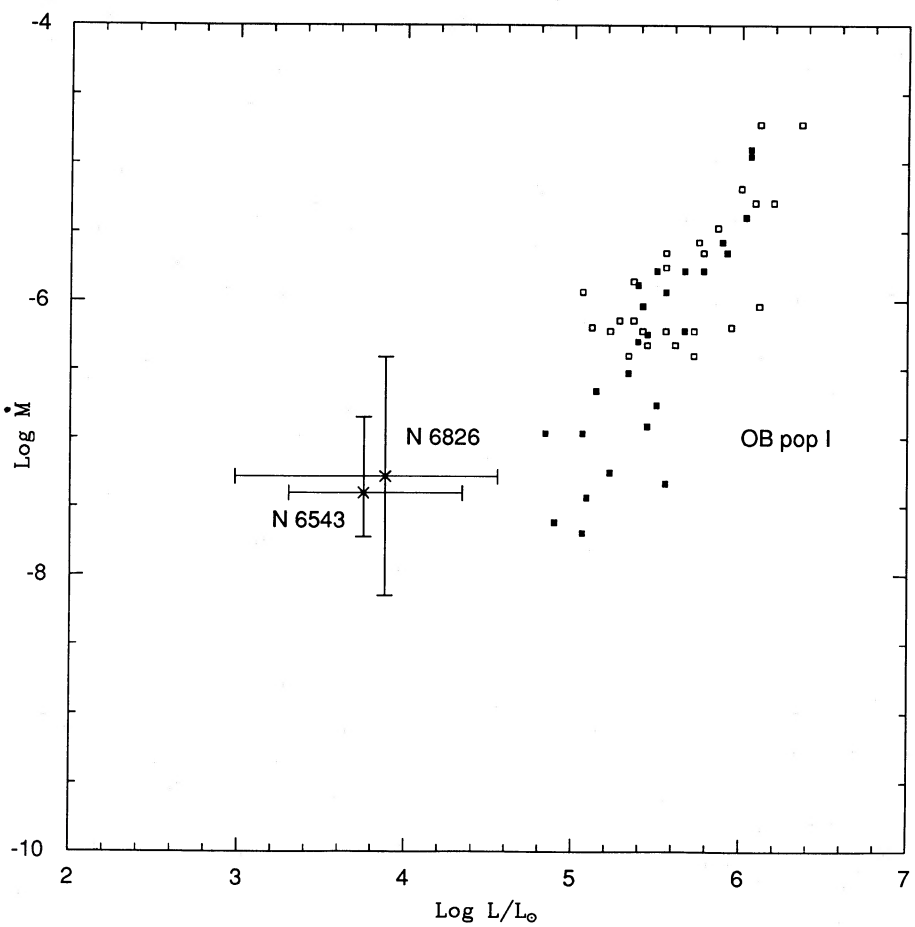

FIG. 14.—Central stars of the planetary nebulae NGC 6543 and NGC 6826 are compared in the [log $\dot{M}$, log $(L/L_\odot)$]-plane with the behavior of Population I OB stars (Garmany and Conti 1984).

© American Astronomical Society • Provided by the NASA Astrophysics Data System

1989ApJ...337..382P

TABLE 9

COMPARISON BETWEEN MASS FLUXES FROM PNCSs AND POPULATION I HOT STARS

Source of Mass Flux	log $(L/L_\odot)$	log T (K)	log $(R/R_\odot)$	log $\dot{M}$ $(M_\odot\ \mathrm{yr}^{-1})$	log F_m $(\mathrm{g\ cm^{-2}\ s^{-1}})$
NGC 6543	3.75 ± 0.50	4.78 ± 0.06	-0.15 ± 0.15	$-7.4 \pm .6$	$-4.1 \pm .6$
Population I	6.5	4.78	1.21	-4.4	-3.8
NGC 6826	3.88 ± 0.80	4.65 ± 0.09	0.16 ± 0.16	$-7.3 \pm .7$	$-4.6 \pm .7$
Population I	5.4	4.65	0.93	-6.2	-5.0

and NGC 6826. In comparison with the authors who have previously studied the two stars with high-resolution *IUE* data, we have used the SEI method, which is physically more complete than the methods used by the other authors, because it accounts for collisional effects and turbulence in the wind. Moreover, we have obtained a better fit of the observed profiles in the various lines.

iv) *Comparison with Population I OB Stars*

We compare the mass-loss rates of the two PNCSs with those of Population I OB stars in a (log $\dot{M}$, log L)-diagram (Fig. 14). The mass-loss rates of the Population I stars are from Garmany and Conti (1984). The two PNCSs are located above the extrapolation of the Population I stars to lower luminosities. The linear best fit of the data points of Population I stars in Figure 14, derived by Garmany and Conti (1984), predicts mass-loss rates of $1.3 \times 10^{-9}\ M_\odot\ \mathrm{yr}^{-1}$ for NGC 6543 and $2.1 \times 10^{-9}\ M_\odot\ \mathrm{yr}^{-1}$ for NGC 6826. This is a factor of 3×10^{-2} smaller than the observed values.

This is not too surprising. The two PNCSs have effective temperatures of 45,000 K and 60,000 K, whereas the OB stars with luminosity log $(L/L_\odot) < 4$ have temperatures below 30,000 K. The extrapolation of the $\dot{M}$-L relation of Garmany and Conti (1984) to such low temperatures is hardly justified. Therefore the comparison between the PNCSs and Population I stars in the $\dot{M}$-L diagram should be made with caution.

It is generally agreed that the mechanism responsible for the fast winds observed in Population I hot stars is the radiation pressure on heavy elements. According to this theory (cf. Abbott 1982; Pauldrach, Puls, and Kudritzki 1986), the mass flux depends on the gravity, on the chemical abundance of heavy elements, and mostly on the temperature. The central stars of NGC 6543 and NGC 6826 have gravities and chemical abundances not much different from those of main-sequence hot stars.

It is therefore interesting to compare the mass fluxes of the PNCSs with those of Population I stars with *the same effective temperatures*. This is shown in Table 9. For the Population I stars we adopted the same temperatures as those of the PNCSs, the radii for the zero-age main sequence, and the mass-loss rates from the $\dot{M}$-L relation of Garmany and Conti (1984). The data in this table show that the mass fluxes from the PNCSs agree within the uncertainty with those expected from Population I stars of the same temperature. This, together with the relation $v_\infty \sim 3v_{\mathrm{esc}}$ as for the Population I stars, clearly suggests that the mass-loss mechanism of the PNCSs is the same as for the Population I stars: radiation pressure.

IV. CONCLUSIONS

Using the SEI method and high-resolution *IUE* data, we have examined the properties of the fast winds exhibited by the central stars of the planetary nebulae NGC 6543 and NGC 6826. A strong effort has been made to evaluate the parameters of the central stars as accurately as possible. Our values of $\dot{M}$ are $(4.0^{+10}_{-2.1}) \times 10^{-8}$ and $(5.2^{+34}_{-4.5}) \times 10^{-8}\ M_\odot\ \mathrm{yr}^{-1}$ for NGC 6543 and NGC 6826, respectively. A comparison with Population I OB stars in the (log L, log $\dot{M}$)-diagram shows that the mass-loss phenomenon in these central stars is very likely due to the same mechanism thought to prevail in early-type stars of Population I, i.e., the radiation pressure on heavy ions.

REFERENCES

Abbott, D. C. 1982, *Ap. J.*, **259**, 282.
Allen, C. W. 1973, *Astrophysical Quantities* (London: Athlone).
Aller, L. H., and Czyzak, S. J. 1979, *Ap. Space Sci.*, **62**, 397.
———. 1983, *Ap. J. Suppl.*, **51**, 211.
Barker, T. 1983, *Ap. J.*, **267**, 630.
Bianchi, L., Cerrato, S., and Grewing, M. 1986, *Astr. Ap.*, **169**, 227 (BCG).
Boeshaar, G. O., Czyzak, S. J., and Aller, L. H. 1974, *Ap. J. Suppl.*, **28**, 335.
Bohlin, R. C., Harrington, J. P., and Stecher, T. P. 1982, *Ap. J.*, **252**, 635.
Bohlin, R. C., Holm, A. V., Savage, B. D., Snijders, M. A. J., and Sparks, W. M. 1980, *Astr. Ap.*, **85**, 1.
Bombeck, G., Koppen, J., and Bastian, U. 1986, ESA SP-263, p. 287.
Brown, R. L., and Mathews, W. G. 1970, *Ap. J.*, **160**, 939.
Capriotti, E. R., and Daub, C. J. 1960, *Ap. J.*, **132**, 677.
Castor, J. I. 1970, *M.N.R.A.S.*, **149**, 111.
Castor, J. I., and Lamers, H. J. G. L. M. 1979, *Ap. J. Suppl.*, **39**, 481.
Castor, J. I., Lutz, J. H., and Seaton, M. J. 1981, *M.N.R.A.S.*, **194**, 547 (CLS).
Cerruti-Sola, M., and Perinotto, M. 1985, *Ap. J.*, **291**, 237 (CP).
Coleman, C. I., Reay, N. K., and Worsik, S. P. 1975, *M.N.R.A.S.*, **171**, 415.
Daub, C. T. 1982, *Ap. J.*, **260**, 612.
French, H. B. 1981, *Ap. J.*, **246**, 434.
———, 1983, *Ap. J.*, **273**, 214.
Friend, D. B., and Abbott, D. C. 1986, *Ap. J.*, **311**, 701.
Garmany, C. D., and Conti, P. S. 1984, *Ap. J.*, **284**, 705.
Harmann, W. R. 1981, *Astr. Ap.*, **93**, 353.
Heap, S. 1981, in *The Universe at Ultraviolet Wavelengths* (NASA CP-2171), p. 415.
Heap, S. R., and Augensen, H. J. 1987, *Ap. J.*, **313**, 268.
Heap, S. R., *et al.* 1978, *Nature*, **275**, 385.
Hummer, D. G., and Mihalas, D. 1970, JILA Rept. No. 101.
Hutsemékers, D., and Surdej, J. 1987, *Astr. Ap.*, **173**, 101.
Iben, I., and Renzini, A. 1983, *Ann. Rev. Astr. Ap.*, **21**, 271.
Kaler, J. B. 1976, *Ap. J. Suppl.*, **31**, 517.
———. 1978*a*, *Ap. J.*, **225**, 527.
———. 1978*b*, *Ap. J.*, **226**, 947.
———. 1981*a*, *Ap. J.*, **249**, 201.
———. 1981*b*, private communication to CLS.
———. 1983, *Ap. J.*, **264**, 598.
———. 1986, *Ap. J.*, **308**, 337.
Koester, D., Schulz, H., and Weidemann, V. 1979, *Astr. Ap.*, **76**, 262.
Lambert, D. L. 1978, *M.N.R.A.S.*, **187**, 1P.
Lamers, H. J. G. L. M., Cerruti-Sola, M., and Perinotto, M. 1987, *Ap. J.*, **314**, 726 (LCP).
Lamers, H. J. G. L. M., and Morton, D. C. 1976, *Ap. J. Suppl.*, **32**, 71.
Liller, W. 1955, *Ap. J.*, **122**, 240.
Liller, W., and Aller, L. H. 1954, *Ap. J.*, **120**, 48.
Mendez, R. H., Kudritzki, R. P., Herrero, A., Husfeld, D., and Groth, H. G. 1988, *Astr. Ap.*, **190**, 113.
O'Dell, C. R. 1963, *Ap. J.*, **138**, 1018.
Parkinson, J. H. 1977, *Astr. Ap.*, **57**, 185.
Pauldrach, A., Puls, J., and Kudritzki, R. P. 1986, *Astr. Ap.*, **164**, 86.
Perinotto, M., and Patriarchi, P. 1980, *Ap. J.*, **238**, 614.
Pottasch, S. R., Preite-Martinez, A., Olnon, F. M., Jing-Er, M., and Kingma, S. 1986, *Astr. Ap.*, **161**, 363.
Pwa, T. H., Mo, J. E., and Pottasch, S. R. 1984, *Astr. Ap.*, **139**, L1.

© American Astronomical Society • Provided by the NASA Astrophysics Data System

1989ApJ...337..382P

Razmadze, N. A. 1956, *Astr. Zh.*, **33**, 3.
———. 1958, *Bull. Abastumani Ap. Obs.*, **23**, 91.
Savage, B. D., and Mathis, J. S. 1979, *Ann. Rev. Astr. Ap.*, **17**, 73.
Surdej, J. 1983, *Astr. Ap.*, **127**, 304.
Tamura, S. 1970, *Sci. Rept. Tohoku Univ.*, **53**, 10.
Torres-Peimbert, S., and Peimbert, M. 1977, *Rev. Mexicana Astr. Ap.*, **4**, 341.
Vorontsov-Velyaminov, B. A., Kostyakova, E. B., Dochuchaeva, O. D., and Arkhipova, V. P. 1965*a*, *Astr. Zh.*, **42**, 464.
———. 1965*b*, *Astr. Zh.*, **42**, 730.
Walborn, N. R., Nichols-Bohlin, J., and Panek, R. J. 1985, NASA Ref. Pub. 1155.

Note added in proof.—During the reading of the proofs a technical mistake was discovered by the authors. The adopted terminal velocity should not have been taken equal to the measured edge velocity (see § III) but to $v_\infty \simeq v_{\rm edge} - 2v_{\rm turb}$, with $v_{\rm turb} = W_{\rm G} v_\infty$. This mistake does not affect the analysis of NGC 6543, due to its very small $W_{\rm G}$ (cf. Lamers, Cerruti-Sola, and Perinotto 1987), while it implies some differences in the analysis of NGC 6826, having $W_{\rm G} = 0.05$. The new best-fitting parameters are $\beta = 2$ for the velocity law and the following pairs of values (T, α_2) for the indicated ions: $(>100, 4)$ for N v; (1, 4) for O IV; (2, 4) for O v; $(\geq 50, 2)$ for C IV; and (0.5, 2) for N IV. With these values the fits of the theoretical profiles to the observed profiles become better than those shown in Figures 9–13, which are relative to the values given in Table 6. The new values of $\dot{M}\langle q_i \rangle$ are: $\geq 6.3(-11)$ for C IV, $2.3(-8)$ for N IV, $>8.7(-9)$ for N v, $5.7(-8)$ for O IV, and $7.4(-9)$ for O v. The values of $\dot{M}\langle q_i \rangle$ for the unsaturated lines are therefore little affected by the reduction of v_∞. The lower limits of $\dot{M}\langle q_i \rangle$ for the saturated lines are reduced by a factor of about 3. The new value of $\dot{M}$ for NGC 6826 is $6.4(-8)\ M_\odot\ {\rm yr}^{-1}$. The discussion and the conclusions remain substantially unchanged.

CERRUTI-SOLA, M.: Osservatorio Astrofisico di Arcetri, Largo E. Fermi, 5, 50125 Firenze, Italy

LAMERS, H. J. G. L. M.: Laboratory for Space Research, Beneluxlaan 21, 3527 HS Utrecht, The Netherlands

PERINOTTO, M.: Istituto di Astronomia, Università di Firenze, Largo E. Fermi, 5, 50125 Firenze, Italy

© American Astronomical Society • Provided by the NASA Astrophysics Data System